Numerical and Experimental Investigation of the Oscillating Wake of a Blunt-Based Body

A. E. FANNING* AND T. J. MUELLER†
University of Notre Dame, Notre Dame, Ind.

The oscillating wake of a blunt-based body is examined using explicit finite-difference solutions of the Vorticity Transport equation and Poisson's equation. The difference equations are formulated for a rectangular grid with varying grid line spacing. Utilization of this type of grid allows increased accuracy to be obtained in the regions of highest gradients, without the large increases in computation time associated with refining a uniformly spaced grid. The accuracy of the numerical solutions was verified, qualitatively, by a comparison with an experimentally obtained flow pattern, and quantitatively, by a comparison with experimentally obtained Strouhal numbers. The basic parameters governing the problem were found to be the thickness and profile of the boundary layers on the body prior to separation, and the Reynolds number. The Reynolds number based on the base height was varied in the range from 100.0 to 16,295.0, while the boundary-layer thickness was varied in the range from 0.121 to 3.0 base heights. The numerical solutions in this area exhibited three types of wake oscillations. The first type of oscillation involved the alternate growth and decay of circulation regions, which remained attached to the base of the body. In the second type of oscillation, the circulation regions would grow in size and eventually detach from alternating sides of the base. The third type of wake oscillation appears to be a more violent version of the second type, again involving growth and detachment of circulation regions from the base of the body. The flow pattern in the third type of oscillating wake closely resembles that of the classic von Kármán vortex street.

Nomenclature

f = arbitrary function
h = base height
L = over-all body length
Re_h = Reynolds number based on base height, $U_\infty h/\nu$
t = time
u = "x" velocity component
v = "y" velocity component
x = Cartesian coordinate
y = Cartesian coordinate
Y = distance above body surface
Δx = grid spacing in "x" direction
Δy = grid spacing in "y" direction
δ = boundary-layer thickness
ν = kinematic viscosity
ζ = vorticity, defined by $\partial v/\partial x - \partial u/\partial y$
ψ = stream function, defined implicitly by $u = \partial\psi/\partial y$, $v = -\partial\psi/\partial x$

Superscript
* = nondimensional

Subscripts
∞ = based on freestream
i,j = state at i,j grid point

Introduction

THE oscillating wake is perhaps one of the most widely studied problems in fluid dynamics. The earliest interest in the problem predates the work of Strouhal[1] on aeolian tones emanating from a wire in an airstream and the most widely cited work is probably von Kármán's[2] model for predicting the spacing ratio of vortices in such a wake. Since these works, many capable investigators have made significant experimental and theoretical contributions to the understanding of this phenomena. However, a solution to the partial differential equations which govern this unsteady flow of a viscous fluid could not be adequately approached prior to the recent refinements of both computational machines and finite-difference techniques. Without such a solution, it was not possible to fully understand the mechanism through which the oscillating wake was formed.

The earliest interest in the oscillating wake had been largely limited to the flow behind circular cylinders, thus it is understandable that the first numerical solutions[3] were obtained for this case. Considerable interest in the oscillating wakes behind other bluff bodies had been generated. Particular interest was generated in the wake of blunt-based airfoils which could provide significant advantages at high speeds, if the drag penalty of the oscillating wake at low speeds could be overcome. Following the inference of Roshko,[4] that a reduction in drag could be accomplished by interfering with the formation process, Wood[5,6] and Bearman[7,8] performed extensive experimental investigations into the effect of base bleed and wake splitter plates on the oscillating wake. In order to fully understand the process by which these methods interfere with the wake formation it would have been most helpful to have a solution to the governing equations which would have shown the details of the undisturbed formation process. The goal of this work is to provide numerical solutions which will enhance the understanding of the mechanism by which an oscillating wake is formed.

This work is essentially an extension of the work of Mueller and O'Leary[9] in which they computed the flowfield associated with a blunt-based body. That work assumed a steady, symmetric solution, thus limiting the Reynolds numbers examined to a maximum of 300, based on the base height.

Numerical Phase

The numerical phase of this work involved formulating the governing equations, constructing a finite-difference mesh to fit

Presented as Paper 71-603 at the AIAA 4th Fluid and Plasma Dynamics Conference, Palo Alto, Calif., June 21–23, 1971; submitted November 15, 1972; revision received May 11, 1973. The authors gratefully acknowledge the efforts of H. Ackert for preparing the figures.

Index categories: Jets, Wakes, and Viscid-Inviscid Flow Interactions; Nonsteady Aerodynamics.

* Teaching Assistant, Department of Aerospace and Mechanical Engineering; presently Staff Member, Aero-Propulsion Laboratory, Wright-Patterson Air Force Base, Ohio. Member AIAA.

† Professor, Department of Aerospace and Mechanical Engineering; presently Visiting Professor, von Kármán Institute for Fluid Dynamics, Rhode-St-Genese, Belgium. Associate Fellow AIAA.

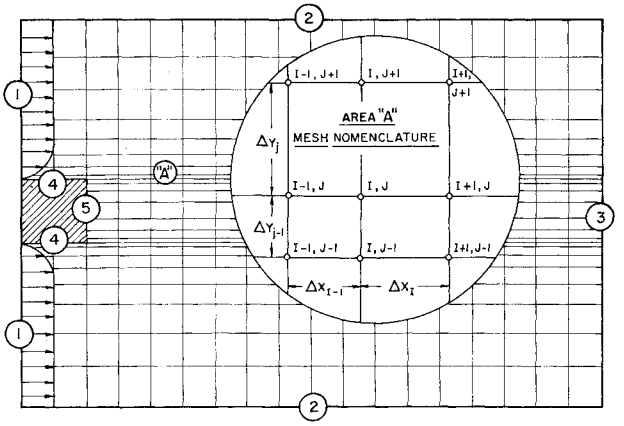

Fig. 1 Variable rectangular grid with enlargement showing grid nomenclature.

the problem, expressing the governing equations in a finite-difference form, setting the initial and boundary conditions, and, finally, solving the resultant system. The solution was in the form of stream function and vorticity fields from which information about the fluctuating velocity field could be extracted.

Governing Equations

Subject to the assumptions of incompressibility and two-dimensionality, the Navier-Stokes equations, in a rectangular Eulerian coordinate system, may be expressed as Poisson's equation and the vorticity transport equation.[10] By nondimensionalizing the components of the equations, it is possible to extend the range of applicability by use of Reynolds principle of similarity. To this end, nondimensionalization is accomplished by the use of the following[10]:

$$\begin{aligned} x &= x^*h & y &= y^*h \\ u &= u^*U_\infty & v &= v^*U_\infty \\ \psi &= \psi^*U_\infty h & \zeta &= \zeta^*U_\infty/h \\ t &= t^*h/U_\infty \end{aligned} \tag{1}$$

The nondimensional vorticity transport equation can be written as

$$\frac{\partial\zeta^*}{\partial t^*}+\frac{\partial u^*\zeta^*}{\partial x^*}+\frac{\partial v^*\zeta^*}{\partial y^*}=\frac{1}{Re_h}\left[\frac{\partial^2\zeta^*}{\partial x^{*2}}+\frac{\partial^2\zeta^*}{\partial y^{*2}}\right] \tag{2}$$

where the nondimensional vorticity and stream function are related by the Poisson equation

$$-\zeta^*=\partial^2\psi^*/\partial x^{*2}+\partial^2\psi^*/\partial y^{*2} \tag{3}$$

Before a finite-difference formulation of these two equations can be made, the finite-difference mesh should be constructed to fit the problem.

Finite-Difference Mesh Structure

In the finite-difference approximation to the solution of the governing equations, approximations to the actual values of the variables are obtained at a finite number of points within the flowfield. When the grid lines are equally spaced in all areas of the flowfield, the spacing is governed by that necessary to obtain the desired accuracy in the area of largest gradients, leading to a high density of grid points in areas where there are low gradients. Fortunately, it is possible, in some cases, to tailor the grid spacing to the particular problem, decreasing the grid point density in the areas of low gradients and increasing this density in the areas of high gradients. This may be accomplished without losing the advantages of a rectangular grid. In the present problem, the largest gradients occur in the boundary layers on the body and in the region one and one-half base heights either side of the centerline, downstream of the base. The finite-difference nomenclature is shown on Fig. 1, which also shows a grid tailored to concentrate points in the locations of large gradients. The grid used during computation was much finer than that of Fig. 1, consisting of 56 grid spaces in the stream-wise direction and 112 grid spaces in the cross stream direction. The nonuniform nature of the mesh structure requires a special formulation of the finite-difference approximations to the partial derivatives.

Finite-Difference Derivatives

In order to formulate the governing equations in finite-difference form, it is necessary to obtain finite-difference expressions for the first and second derivatives. Standard Taylor series expansions yield[10] for the first derivative in the x direction

$$\frac{\partial f_{i,j}}{\partial x}=\frac{\Delta x_{i-1}f_{i+1,j}}{\Delta x_i(\Delta x_{i-1}+\Delta x_i)}-\frac{\Delta x_i f_{i-1,j}}{\Delta x_{i-1}(\Delta x_{i-1}+\Delta x_i)}-\frac{(\Delta x_{i-1}-\Delta x_i)f_{i,j}}{\Delta x_i\Delta x_{i-1}} \tag{4}$$

and for the second derivative in the x direction

$$\frac{\partial^2 f}{\partial x^2}=\frac{2f_{i+1,j}}{\Delta x_i(\Delta x_{i-1}+\Delta x_i)}+\frac{2f_{i-1,j}}{\Delta x_{i-1}(\Delta x_{i-1}+\Delta x_i)}-\frac{2f_{i,j}}{\Delta x_i\Delta x_{i-1}}-\frac{(\Delta x_{i-1}-\Delta x_i)}{3}\frac{\partial^3 f}{\partial x^3}-\frac{\Delta x_i\Delta x_{i-1}}{24}\frac{\partial^4 f}{\partial x^4} \tag{5}$$

If this last expression is truncated before the term containing $\partial^3 f/\partial x^3$, the approximation is not necessarily accurate to the order of magnitude of (Δx^2). However, if the grid is constructed in such a fashion that the order of magnitude of $(\Delta x_{i-1}-\Delta x_i)$ is the same as the order of magnitude of $(\Delta x_{i-1}\Delta x_i)$ truncation prior to this term is permissible, while limiting truncation errors to the order (Δx^2). In this specific case, the expression for $\partial^2 f/\partial x^2$ is given as

$$\frac{\partial^2 f}{\partial x^2}=\frac{2f_{i+1,j}}{\Delta x_i(\Delta x_{i-1}+\Delta x_i)}+\frac{2f_{i-1,j}}{\Delta x_{i-1}(\Delta x_{i-1}+\Delta x_i)}-\frac{2f_{i,j}}{\Delta x_i\Delta x_{i-1}} \tag{6}$$

The derivations of $\partial f/\partial y$ and $\partial^2 f/\partial y^2$ are completely analogous to the above derivations with Δx replaced by Δy, and the index j varying.

Boundary and Initial Conditions

In the solution of any time dependent partial differential equation, it is necessary to specify the conditions on the boundaries of the system and the initial state of the system.

Upstream mesh boundary

At the inflow or upstream boundary, surfaces 1, Fig. 1, two different boundary conditions were applied. Generally, a Pohlhausen profile of the proper thickness was specified for the boundary layer and the resultant velocity profile was integrated to obtain values of the stream function on the inflow boundary. In one case the velocity profile was obtained experimentally and integrated to provide the necessary stream function values. The vorticity on this boundary was computed directly from Poisson's equation, using a centered difference in the y direction and a forward difference in the x direction.

Upper and lower mesh boundaries

The upper and lower mesh boundaries, surfaces 2, Fig. 1, were assumed to be undisturbed stream lines. The actual condition at an infinite distance from the body was thus brought to within a finite distance of the body. This was felt to be an acceptable boundary condition as Mueller and O'Leary[9] have shown that the lid location has little effect, if it is farther than three and one-half base heights from the centerline. Further following the approach of Roache and Mueller,[11] the vorticity

was specified as equal to the vorticity one grid space within the mesh.

Downstream mesh boundary

Determining the boundary condition to be applied at the downstream boundary, surface 3, Fig. 1, presents a difficult problem. The distribution of values on this surface must be known in order to solve the problem. However, in the current problem, there is no proper way of determining this distribution. It should be noted that each distribution, which satisfies the governing equation and any appropriate auxiliary conditions, will yield a solution to the problem. If the downstream boundary is sufficiently far removed from the region of interest, then the solutions will differ only slightly in that region of interest, and any of the various solutions will provide an adequate approximation to the actual solution. Several methods of specifying the outflow distribution were attempted,[12] although a linear extrapolation was finally chosen as the least restrictive. This method was used to determine both vorticity and stream function on the downstream boundary.

Body surfaces

As the stream function on the body surface was chosen to be identically zero there was never any need to recompute this value. Following the work of Roache and Mueller,[11] the vorticity on surfaces 4 and 5, Fig. 1, was computed using a one sided difference, thus the corner points were assigned two values of vorticity. While computing a point above or below the corners, the corner was treated as if it lay on the upper or lower surface, respectively. However, while computing a point behind the base, the corner was treated as if it lay on the base of the body.

Initial conditions

Three types of initial conditions were used successfully. The first defined the stream lines as parallel, straight lines, upstream of the base, which were turned through an angle at the plane of the base and projected to the downstream boundary. The second defined the stream lines to be parallel to the centerline both upstream and downstream of the plane of the base. At the base, the stream lines underwent a sharp vertical deflection. In both of these initial conditions a slight asymmetry was introduced by deflecting the zero stream line one grid point vertically from the centerline. The third condition was the use of a previously attained solution as the starting point for a new case.

Method of Solution

An upwind differencing technique given by Roache and Mueller,[11] was applied to the vorticity transport equation, and an explicit differencing scheme was used to determine the vorticity value at each interior grid point, at a new time. Compatible values of the stream function were obtained by solving the Poisson equation by an iterative technique called successive over-relaxation.[13] Once the solution to Poisson's equation was obtained, the boundary conditions on vorticity were recomputed and the sequence restarted at the calculation of vorticity at a new time level. The repetition of this sequence continued until the flow pattern repeated itself at a definite frequency. The oscillatory solution was then considered to have been reached.

Interpretation of Plotted Fields

Nearly all results from the numerical phase of this work are presented as contour plots of the stream function, i.e., streamlines. This method of presenting the results was chosen as it enhanced the investigators' understanding of the flowfield. Only the portion of the grid, which is required to observe the region of interest, is presented. The plots therefore, do not necessarily represent the entire calculated field. The plots presented in this work represent only a small fraction of those obtained during the investigation. The increments in stream function between adjacent plotted streamlines were not uniform throughout the plotted field. Rather, they were chosen to best demonstrate the character of the flow and minimize plotting time.

A bifurcation of the zero streamline, where it separates from the body, is evident in nearly all plots. This bifurcation is not indicative of two separation points. Rather, it is a characteristic of the plotting routine and the limits of the solution. The finite-difference solution can not locate the position of separation, it can only specify the two grid points on the body between which separation occurs. In a manner consistent with this limit of the solution, the plotting routine draws a line to both grid points. The point of separation, then lies between the two intersections with the body.

Experimental Phase

The experimental phase of this work was divided between two Reynolds number ranges. In the high Reynolds number range, Strouhal number and velocity profile data were compiled. In the low Reynolds number range, the flow patterns were photographed for comparison with the computed patterns.

Low Reynolds Number Experiments

The experimentation in this Reynolds number range, $Re_h \simeq 500$, was designed to yield path line photographs of aluminum particles suspended in a water channel through which the model was towed.[10] As the photographs were time exposures, the aluminum particles appeared as streaks. These streaks define the paths of the particles, during the time interval in which the film was exposed. When these streaks are straight lines, or approximately so, the velocity vector must lie tangent to the path line. Since the velocity vector must also lie tangent to a streamline, a comparison with the streamline plots of the numerical phase is possible.

During the experiment, it was noted that the two-dimensional assumption was valid only in the near wake. Since the numerical results were very strongly dependent upon the two-dimensional assumption, the region of meaningful comparison was limited to the region within 2 base heights downstream of the base. Further downstream, a three-dimensional swirling motion developed as had been noted earlier by Mueller and O'Leary.[9]

High Reynolds Number Experiments

The experimentation in the Reynolds number range, $Re_h \simeq 1.6 \times 10^4$ was designed to yield: a velocity profile at the same location as the inflow boundary of the finite-difference grid; the wake Strouhal number; and the freestream Reynolds number. The determination of these parameters enabled a direct comparison of identical numerical and experimental cases. These experiments were conducted in one of the University of Notre Dame's low-speed, low-turbulence wind tunnels, fitted with a DISA hot-wire probe.[10] The experimental procedure involved traversing the flowfield along the inflow station, thereby obtaining the freestream velocity and the velocity profile at the inflow station, and traversing the wake to determine the frequency of oscillation of the wake. As in the experimental work of Bearman,[7,8] although traversals were made at various locations in the wake, the location of optimum signal clarity was found to be one base height downstream of the base and one base height distant from the centerline. The frequency was taken to be the average frequency recorded at this location over a 10-sec measuring period.

Discussion of Results

Once the problem has been properly formulated, it is evident that for a given geometry only three parameters can affect the

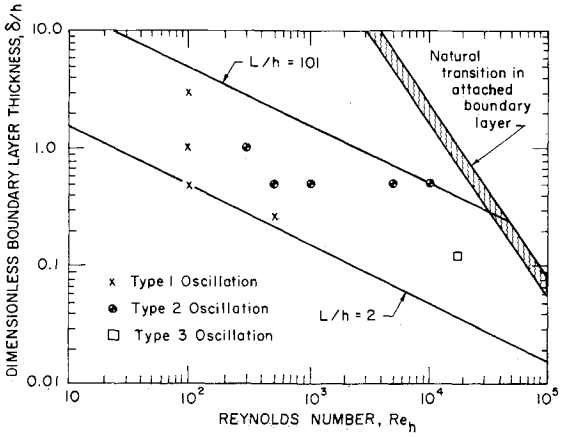

Fig. 2 Combinations of δ/h and Re_h corresponding to practical cases, and types of wake oscillations.

solution. These are the velocity profile at the inflow station, the thickness of the boundary layer on the surface of the body at the inflow station, and the freestream Reynolds number. With the one exception noted earlier, all cases presented in this work used a Pohlhausen profile at the inflow station. Thus, only δ/h and Re_h, needed to be varied to examine all possible solutions for this problem. The theoretical combinations of δ/h and Re_h are limitless but fortunately only a limited range of these combinations is of interest. If a Blasius type boundary-layer growth upstream of the inflow station is assumed, it is possible to relate both these factors to a single geometric parameter, L/h, the ratio of the over-all length to the base height. Limiting the bodies of interest to those where this parameter is greater than 2 and less than 101, defines a band of practical interest on a plot of δ/h vs Re_h. An upper bound may be placed on the Reynolds number by considering where natural transition occurs. The region thus defined is shown on Fig. 2. Within this region, three types of oscillating wakes were noted when the solutions were computed and these were marked as to which type of oscillation occurred. All numerical solutions were obtained using a Univac 1107 digital computer.

In the first type of oscillating wake, which was noted, a small amplitude oscillation in the size of the circulation regions, attached to the base occurred. The limiting points of this type of oscillation are shown in Fig. 3a and 3b. Mueller and O'Leary[9] had assumed the flowfield to be symmetric and therefore this oscillation was not noted in their work.

The plotted results indicate that the regions of circulation are not enclosed by stream lines separating from the base and rejoining downstream of the circulation regions. It appears that a region at the trailing edge of the circulation regions allows fluid from the shear layer, separated from one side of the base, to enter the region of circulation on the other side. Thus there is mass transfer across the wake even in this attached state. The small "gate" through which this interaction is allowed, oscillates

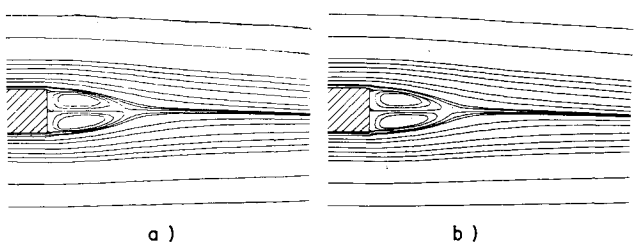

Fig. 3 Flow patterns showing limits of first type of wake oscillation, $Re_h = 100.00$, $\delta/h = 0.5$, plotted values of $\psi = (0.00, \pm 0.0125, \pm 0.025, \pm 0.05, \pm 0.1, \pm 0.2, \pm 0.3, \pm 0.4, \pm 0.5, \pm 1.0, \pm 1.5)$.

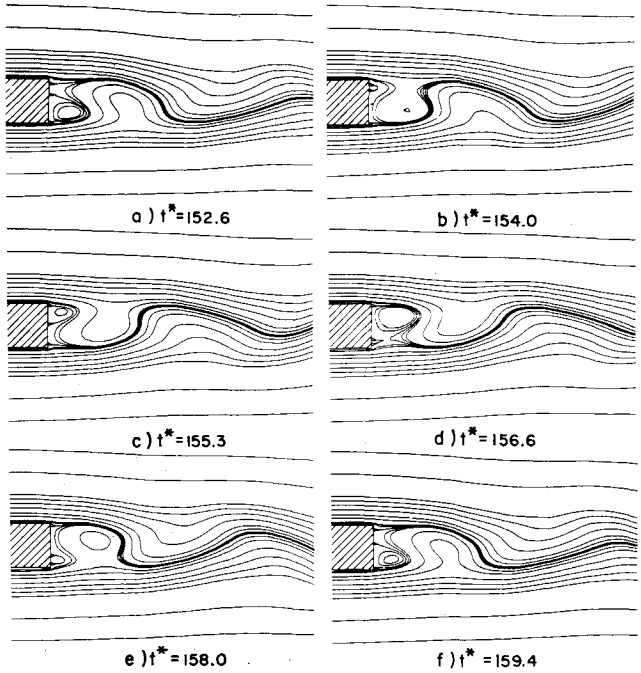

Fig. 4 Flow patterns at various times during one period of the second type of wake oscillation, $Re_h = 500.0$, $\delta/h = 0.5$, plotted values of $\psi = (0.00, \pm 0.0125, \pm 0.025, \pm 0.05, \pm 0.1, \pm 0.2, \pm 0.3, \pm 0.4, \pm 0.5, \pm 1.0, \pm 1.5)$.

from one side to the other. It appears that this interaction between the region of circulation on one side and the shear layer on the other side plays an integral part in maintaining the oscillation. This oscillation would otherwise be expected to diminish due to the viscous interaction between the two circulation regions. This natural oscillation, if it were to amplify at a higher Reynolds number, could mean that no other perturbation would be necessary to cause the circulation regions to detach and move downstream.

The second type of oscillating wake, noted during the investigation, involved the growth and subsequent detachment of circulation regions from alternate sides of the base, as shown in Fig. 4, and appeared to be an outgrowth of the first type of oscillation. The higher Reynolds number apparently caused the oscillatory circulation regions to grow outside the limit within which the first type was stable. That this limit is related to the boundary-layer thickness was demonstrated by the return to the first mode of oscillation when the boundary-layer thickness was halved.[12] The second type of oscillation was re-established upon returning the boundary layer to the original thickness and was also established starting from a different set of initial conditions.[10] In passing from the first type of oscillation to the second type, the circulation regions continued to oscillate relative to each other while becoming elongated. The elongation continued until a phenomenon called stream line capture by Thompson[14] occurred. Stream line capture consists of a stream line which passes over one side of the body, looping around the downstream side of the circulation region on the near side and the upstream side of the one on the far side, before continuing downstream. More stream lines were entrained into the circulation region and the circulation region moved downstream from the base. Part of the region was, however, squeezed off and left behind to form the core of a new circulation region. After a circulation region moved downstream, the stream lines from the side of the body where it formed were entrained into the circulation region on the other side of the body. As time progressed this sequence became more firmly established,[10] and assumed a definite frequency. This solution is quite similar in character to that presented by Thoman and Szewczyk[3] for flow over a stationary cylinder at a Reynolds number of 200, based

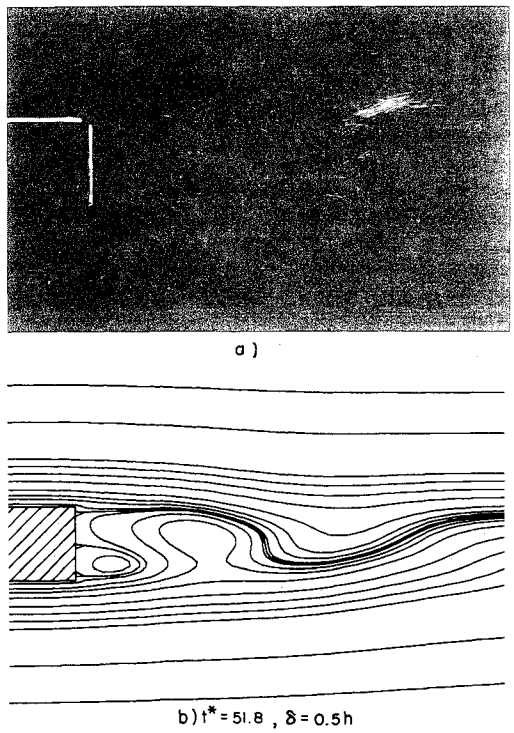

Fig. 5 Qualitative comparison between experimental and numerical flow patterns, $Re_h = 500.0$, $\delta/h = 0.5$, ψ values plotted = (0.00, ±0.0125, ±0.025, ±0.05, ±0.1, ±0.2, ±0.3, ±0.4, ±0.5, ±1.0, ±1.5).

on the cylinder diameter. One characteristic of the second mode is that the disturbance of the freestream in the region of circulation formation and detachment is minimal. The effect of the large circulation regions in this area is discernible only about three-quarters of a base height above or below the centerline.

In order to verify the accuracy of the numerical solution, it is helpful to compare a computed flow pattern, with the flow pattern obtained experimentally at a comparable Reynolds number and boundary-layer thickness. Fig. 5a shows a fully established flow pattern. Immediately evident is a large circulation region centered approximately 1.5 base heights downstream of the base and 0.25 base heights above the centerline. The particle paths in the region above the centerline and very near the base show evidence of being in this circulation region. A smaller circulation region has begun to form on the lower portion of the base. A comparison with the plot of Fig. 5b shows the same prominent features and indicates that the large circulation region does extend to the base. Thus verifying the numerical result, at least in a qualitative sense.

In an effort to duplicate, numerically, the situation of the high Reynolds number experiment, the velocity profile was assigned to agree with the results of the experiment,[10] the boundary-layer thickness was set to be $0.121h$, and the Reynolds number was set to be 16,295, these values being determined from the experiment. The third type of oscillating wake, resulted from these parameters. During the computation of this case, a finer mesh was used and a stricter convergence criteria was applied. Plots of the flowfield at various times during one period of the oscillation are shown in Fig. 6. This third type of oscillation is distinguished from the second type by the strength of its circulation regions and the extent of their effect. A small region of circulation forms on one side of the base. Driven by the separated shear layer, this circulation gains strength and grows. Its major direction of growth is not downstream, as in the previous cases, but, rather, across the base. Upon interacting with the shear layer on the side of the base, it entrains the fluid in the shear layer, and continues to grow in a cross stream direction. It entrains the flow at a distance of one and one-half base heights from the centerline, prior to reaching a downstream length of one and one-half base heights. By the time the next recirculation region is discernible on the base, the effect of the circulation is evident two base heights from the centerline on the side of flow entrainment into the circulation region. While the initial impression is one of a violently oscillating wake, the stream line pattern appears strikingly similar to that of a von Kármán vortex street, viewed with the body at rest.

Unlike the previous cases, this solution frequently results in separation on the upper or lower surface of the body. It is thus verified that the boundary condition used at the corner did not force separation on the base of the body, but allowed it to occur wherever the situation demanded.

The criterion for transitioning of the free shear layer presented by Roshko and Lau[15] indicates that the shear layers should transition prior to the formation of the detached circulation regions in the case during which this third type of oscillation was obtained. It appears, however, that the finite-difference solution continues to closely approximate the gross flow patterns of the wake, even though it does not take this transitioning into account. For this type of oscillation, at $Re_h = 16{,}295$, the numerically determined Strouhal number ranged between 0.202 and 0.222 compared to the experimental value of 0.259.

Solutions at additional values of the parameters δ/h and Re_h were computed and the type of oscillation corresponding to the additional solutions is noted on Fig. 2 for each case. The boundaries between the different types of oscillations were not sharp but rather one type blended smoothly into the next. The boundaries could not be better defined because this would have required a prohibitively large amount of computer time. Indeed, it is not even definite that all possible types of wake oscillation have been found.

Conclusions

A rectangular grid of varying grid line spacing was devised in order to concentrate grid points in the regions of highest gradients. Using this type of grid, the accuracy of a finite-difference solution was increased with lesser increases in computational times, than if a grid of uniformly spaced lines had

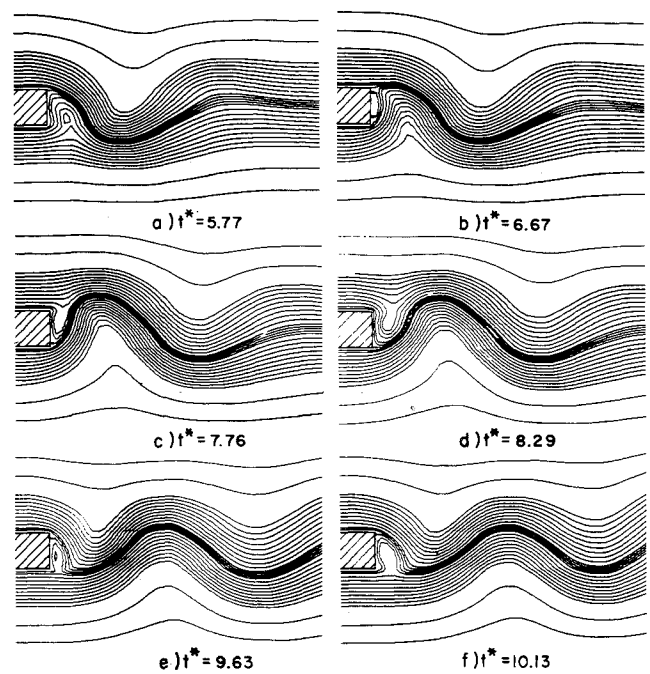

Fig. 6 Flow pattern at various times during one period of the third type of wake oscillation, $Re_h = 16{,}295.0$, $\delta/h = 0.1210$, plotted values of ψ = (0.00, ±0.05, ±0.1, ±0.2, ±0.3, ±0.4, ±0.5, ±0.6, ±0.7, ±0.8, ±0.9, ±1.0, ±1.5, ±2.0).

been used. The finite-difference formulation of the governing differential equations formed a second-order accurate, stable, and thus convergent system, when the appropriate boundary conditions were applied.

The accuracy of the qualitative aspects of the computed solutions was verified by the comparison between computed flow patterns and experimentally obtained flow patterns at a $Re_h \simeq 500$. Excellent agreement was found during this comparison. The quantitative accuracy of the computed solutions was demonstrated by computing the flowfield for one case in which all controllable factors were set equal to those determined during an earlier wind-tunnel experiment and then comparing the numerically obtained Strouhal number, 0.202–0.222, with the experimentally determined one, 0.259. Reasonably good agreement was found during this comparison.

When this system of solution was applied to the problem of the oscillating wake of a blunt-based body, three types of oscillations were found to occur. The first of these involved the alternate growth and decay of two regions of circulation, which remained attached to the base of the body. The second type appeared to be an outgrowth of the first, which became unstable resulting in the growth and subsequent detachment of regions of circulation, vortices, from alternate sides of the base. The boundary between the first and second types of wake oscillation was found to depend strongly on both the Reynolds number and the thickness of the boundary layers on the body prior to separation. The third type of oscillation, although similar to the second, involved a more violent growth and detachment process. The resultant flow pattern was more nearly like that of von Kármán's vortex street.

The growth of the circulation regions appears to result from the viscous interaction between the circulation region and the shear layer separated from the same side of the body. Detachment of these circulation regions is effected by interaction with the shear layer separated from the opposite side of the base.

References

[1] Strouhal, V., "Über eine besondere Art der Tonerregung," *Annalen der Physik und Chemie*, New Series, Vol. 5, 1878, pp. 216–251.

[2] von Kármán, Th. and Rubach, H., "Über den Mechanismus des Flüssigkeits—and Luftwider standes," *Physik Zeitschrift*, Vol. 13, 1912, pp. 49–59.

[3] Thoman, D. C. and Szewczyk, A. A., "Numerical Solutions of Time Dependent Two-Dimensional Flow of a Viscous Incompressible Fluid over Stationary and Rotating Cylinders," TR 66-14, July 1966, Heat Transfer and Fluid Mechanics Lab., Dept. of Mechanical Engineering, Univ. of Notre Dame, Notre Dame, Ind.

[4] Roshko, A., "On the Drag and Shedding Frequency of Two-Dimensional Bluff Bodies," TN 3169, July 1954, NACA.

[5] Wood, C. J., "The Effect of Base Bleed on a Periodic Wake," *Journal of the Royal Aeronautical Society*, Vol. 68, July 1964, pp. 477–482.

[6] Wood, C. J., "Visualization of an Incompressible Wake with Base Bleed," *Journal of Fluid Mechanics*, Vol. 29, Pt. 2, 1967, pp. 259–272.

[7] Bearman, P. W., "Investigation of the Flow Behind a Two-Dimensional Model with a Blunt Trailing Edge and Fitted with Splitter Plates," *Journal of Fluid Mechanics*, Vol. 21, Pt. 2, 1965, pp. 241–255.

[8] Bearman, P. W., "The Effect of Base Bleed on the Flow Behind a Two-Dimensional Model with a Blunt Trailing Edge," *The Aeronautical Quarterly*, Vol. xviii, Aug. 1967, pp. 207–224.

[9] Mueller, T. J. and O'Leary, R. A., "Physical and Numerical Experiments in Laminar Incompressible Separating and Reattaching Flows," AIAA Paper 70-763, Los Angeles, Calif., 1970.

[10] Fanning, A. E., "A Numerical and Experimental Investigation of the Oscillating Flow in the Wake of a Blunt Based Body," M.S. thesis, Aug. 1970, Univ. of Notre Dame, Notre Dame, Ind.

[11] Roache, P. J. and Mueller, T. J., "Numerical Solutions of Compressible and Incompressible Laminar Separated Flows," AIAA Paper 68-741, Los Angeles, Calif., 1968; also *AIAA Journal*, Vol. 8, No. 3, March 1970, pp. 530–538.

[12] Fanning, A. E. and Mueller, T. J., "A Numerical and Experimental Investigation of the Oscillating Flow in the Wake of a Blunt Based Body," AIAA Paper 71-603, Palo Alto, Calif., 1971.

[13] Smith, G. D., *Numerical Solution of Partial Differential Equations*, Oxford University Press, New York, 1965.

[14] Thompson, J. R., "Computer Experimentation with an Implicit Numerical Solution of the Navier-Stokes Equations for an Oscillating Body," AIAA Paper 69-185, New York, 1969.

[15] Roshko, A. and Lau, J. C., "Some Observations on Transition and Reattachment of a Free Shear Layer in Incompressible Flow," *Proceedings of the 1965 Heat Transfer and Fluid Mechanics Institute*, Los Angeles, Calif., June 21–23, 1965.